International Journal of Mechanical Engineering and Robotics Research

ISSN 2278 – 0149 www.ijmerr.com
Vol. 2, No. 4, October 2013

Research Paper

THE EFFECT OF VORTEX GENERATORS ON PRESSURE AND SKIN FRICTION IN A DIFFUSER

Ghobad Shafiei Sabet[1], S Pavithran[1]* and R R Kulkarni[1]

*Corresponding Author: S Pavithran, ✉ vspavitra@gmail.com

The experimental investigation of flow analysis in a diffuser using protrusion and vortex generators is carried out. Two diffuser angles are looked into. One pair protrusion and one and two vortex generator pairs are considered. The velocity profile at the diffuser inlet is uniform and the flow is a developing one. The protrusion and vortex generators are placed near the diffuser inlet. The Reynolds number based on the diffuser length is in the range 2.3-3.6 × 10^5. It is seen that the pressure coefficient is lower for the rough case, compared to the smooth one. It increases with the diffuser angle, as the pressure rise is higher. It also increases with Re. The skin friction coefficient decreases with Re. The smooth case has a lower value. It is higher for the case with a higher diffuser angle. The parallel configuration of protrusion yields the maximum value. It also decreases with the protrusion angle.

Keywords: Skin friction coefficient, Pressure coefficient, Diffuser, Protrusions, Vortex generator

INTRODUCTION

The effect of Vortex Generators (VGs) and protrusions has been looked into in the recent past. Von Stillfried *et al.* (2011) showed the use of two dimensional statistical passive vortex generators model, applied to an adverse pressure gradient boundary layer flow. They showed the vortex generators model's capability to predict flow control sensitivity with respect to the stream wise position.

Biswas *et al.* (1989) performed, one of the first numerical works on vortex-induced heat exchanger enhancement by investigating the impact on mixed convection 'in a rectangular channel. Calculations were performed at Reynolds numbers of 500 and 1815 with Grashof numbers of 0, 2.5E5, and 5.0E5.They evaluated the impact of a single delta wing with an aspect ratio of one and angles of attack of 20° and 26°. The wing was attached to the bottom wall of the channel by its trailing edge. It should be noted that this study did not include the hole under the wing which would result from its being punched out of a fin.

[1] Department of Mechanical Engineering, Vishwakarma Institute of Technology, Pune, India.

Biswas and Chattopadhyay (1992) determined numerically as an extension of earlier work, the structure of flow and heat transfer characteristics in a rectangular channel with a built-in delta wing protruding from the bottom wall. They computed the numerical solution of complete Navier-Stokes and energy equations. They looked into the effect of a punched hole, beneath the wing-type vortex generator, on the heat transfer and skin friction characteristics has been determined. They investigated influence of the vortex generator's angle of attack and Reynolds number on heat transfer and skin friction. They showed average Nu number increases as large as 34% at an angle of attack of 26°.

Fiebig *et al.* (1989) extended their earlier work by evaluating the impact of vortex generation in channel flows. Delta and rectangular wings and winglets were evaluated using the unsteady, liquid crystal thermography technique for aspect ratios varying from 0.8 to 2.0, angles of attack varying from 10° to 60°, and Reynolds numbers varying from 1000 to 2000. They looked into heat transfer and drag results. In these experiments, the pressure drop was so low that the authors chose to measure changes in drag force on a specimen suspended in the wind tunnel. They mentioned numerical results that report the error associated with their implicit equating of drag and total pressure drop to be less than 6%.

Tiggelbeck *et al.* (1992) investigated using the same flow visualization and unsteady liquid crystal thermography techniques. This research was further extended to include two aligned rows of delta winglets. They reported that the qualitative flow structure, the number of developing vortices per vortex generator, and their stream wise development were found to be nearly independent of the oncoming flow of the vortex generator (uniform or vertical). In other words, the second row of vortex generators performed very much like the first row. The local heat transfer enhancement was highest behind the second row of generators, but the effect of the enhancement decreased faster in the stream wise direction for the second row of generators than for the first row. For a Reynolds number of 5600, local heat transfer enhancements of several hundred percent were reported, and the average heat transfer was increased 77% by two aligned rows of vortex generators. No pressure drop data were recorded.

Tiggelbeck *et al.* (1993) extended this multiple row vortex generators work by including staggered vortex generators and pressure drop experiments. Again, the qualitative flow structure, number of vortices per generator, and stream wise development were reported to be nearly independent of upstream flow conditions. The staggered arrangement gave slightly lower heat transfer enhancements than the inline arrangement, but the staggered pressure drop was also lower than the inline arrangement. The average heat transfer was increased 80% for an angle of attack of 45° at Reynolds number of 6000.

Sohankar (2007) presented the flow and thermal simulation using LES and DNS for a channel with two angled ribs forming a vee-shaped vortex generator to augment heat transfer. The Reynolds number was chosen between 200 and 2000 and the incidence angle between 10 and 30. It was reported that

Nusselt number, pressure coefficient, bulk temprature, friction factor and Colburn factor very significantly with the Reynolds number and the incidence angle.

EXPERIMENTAL SETUP AND PROCEDURE

The investigation is carried out in the experimental set up as shown in Figure 1. The diffuser has a cross sectional area of 43 mm × 63 mm at the outlet. A centrifugal blower having a capacity of 1 KW is discharging air from the blower through a flow valve. There is a convergent section just before the diffuser, ensuring uniform flow at diffuser inlet. The working fluid is air.

Diffuser, Protrusion and Vortex Generators Shapes

The geometry of the diffuser is as shown in Figures 2a to 2c. The half angle of the diffuser is denoted as . Two cases, = 5.7° and = 7° are considered.

Figure 1: Experimental Setup

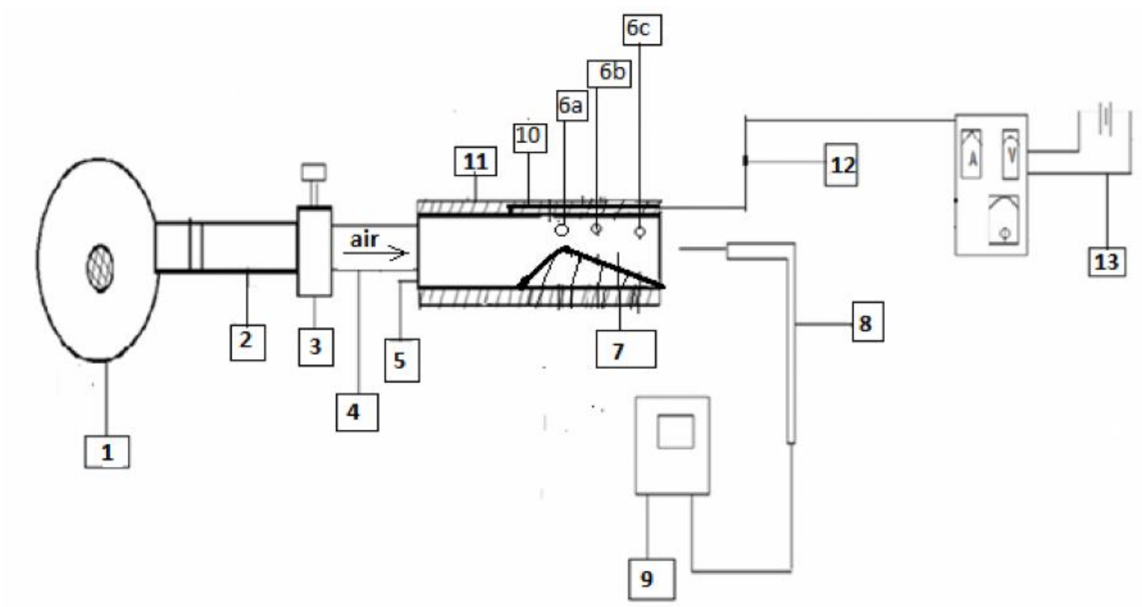

Note: 1. Blower, 2.Connecting pipe, 3. Flow control valve, 4. Pipe, 5. Test section, 6a-c. Static pressure taps for differential manometer, 7. Diffuser, 8. Pitot tube, 9. Digital manometer, 10. Heater, 11. Glass-wool and asbestos rope, 12. Heater electrical wires, 13. Instrument panel main connections.

Figure 2: a) Smooth Diffuser, b) Diffuser Outlet: Side View and c) Diffuser with Protrusion

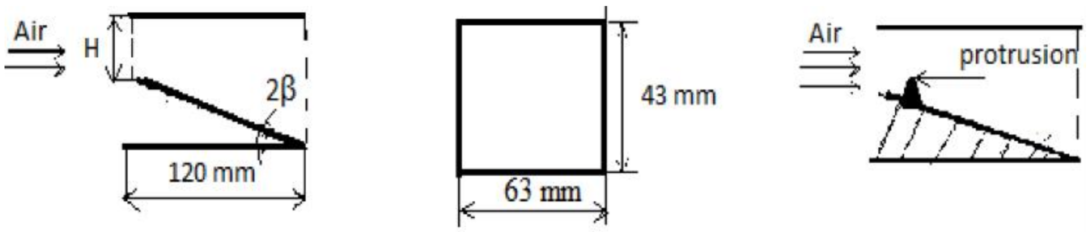

Note: *H* = 18 mm for = 5.7° and *H* = 13 mm for = 7.0°.

Protrusions Shapes

For making the diffuser surface rough, protrusions are glued near the inlet section. The protrusion pairs with the angle of attack ~ = 35° (as shown in Figure 3) are employed. The protrusions have a thickness of 0.5 mm.

The angle made by protrusion pair is denoted as ϒ. This is zero for the parallel case (Figure 4a) negative for the divergent case (Figure 4b) and positive for the convergent one (Figure 4c).

Figure 3: Protrusion with Angle of Attack ~ = 35°

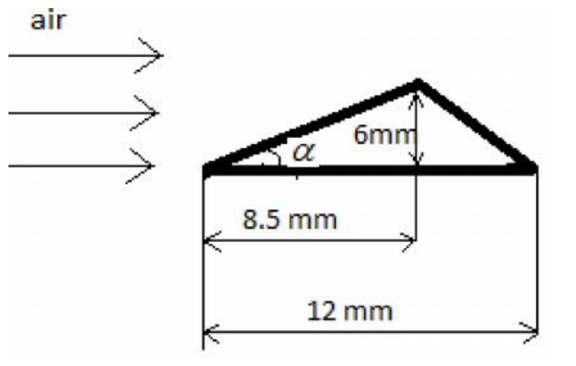

Figure 4: a) Parallel Pair, b) Divergent Pair, and c) Convergent Pair Protrusion (Top View)

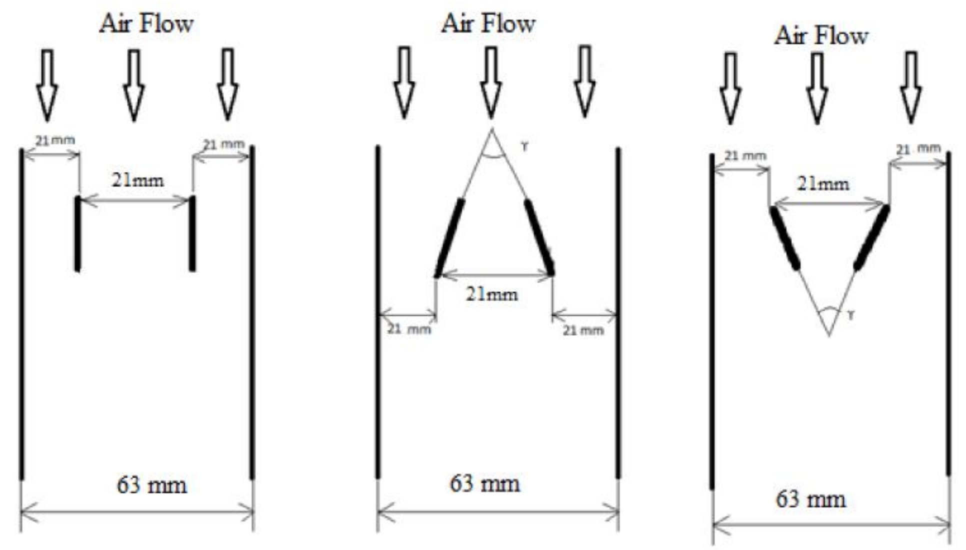

The top view of the diffuser roughened by one pair protrusion is presented in Figures 4a to 4c.

The front view of the diffuser roughened by protrusion is shown in Figure 5.

Figure 5: Diffuser with Protrusion (Front View)

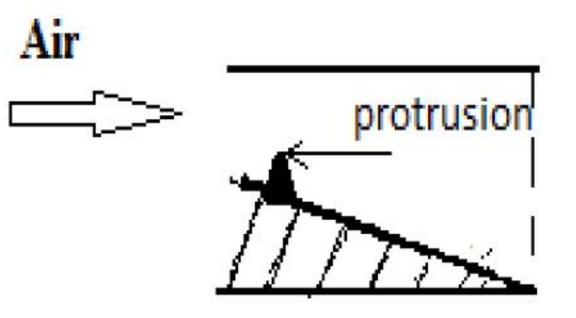

Vortex Generators Shapes

For making the diffuser surface rough, as shown in Figure 6, two pairs VGs (triangular shape, 1 cm each side) are glued near the inlet section on the bottom side. The angle of attack

Figure 6: Diffuser with a) One Pair VGs (Top View), b) Two Pairs VGs (Top View), and c) Two Pair VGs (Front View)

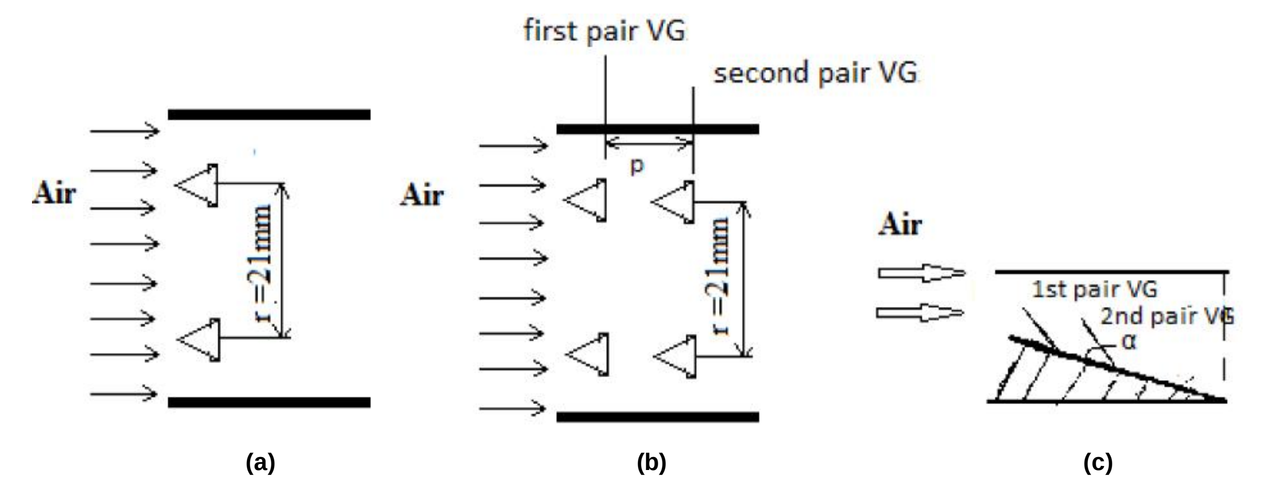

of VGs (~) varies from 19° to 43°. The VGs have a thickness of 0.5 mm.

Pitch of VG (for the two pair case): P = 13 mm

RESULTS AND DISCUSSION

The effect of one pair protrusion and one and two pair vortex generator angles and Re on the diffuser pressure coefficient (C_p) and average skin friction coefficient (C_f) are presented. Two diffusers with half angle 5.7° and 7.0° are considered. The angle of attack of the vortex generator is varied from 19-43°. The inlet velocity varies from 30-45 m/s. For the 7.0° diffuser, the range of Reynolds number based on inlet velocity and diffuser length is in the range 2.8-3.6 and for the one with 5.7°, it varies from 2.3-3.5 × 10^5. The velocity profile is obtained using pitot tube and mass flow rate by numerical integration of the velocity profile.

Experimental Uncertainties

The variables measured are static and stagnation pressures. Pressure is measured by a digital manometer with an uncertainty of ± 0.5 mm of water. The velocity profile is obtained using a pitot tube. The uncertainty in the mass flow rate is 2.5%.

Pressure Coefficient

The pressure coefficient is defined as:

$$C_P = \frac{P - P_{ref}}{\frac{1}{2}\rho V_{in}^{2}}.$$

The inlet pressure is taken as the reference pressure P_{ref}.

From inlet to outlet pressure increases and hence pressure coefficient also increases. The variation of C_p are shown in Figure 7. The variation is similar to that of Von Stillfried *et al.* (2011).

The pressure coefficient C_p increases with Re. This is due to the fact that the losses (as a fraction $\frac{1}{2}\rho V_{in}^{2}$) are lower. The C_p value is lower for the rough case, as the losses are higher.

The effect of diffuser angle on C_p is presented in Figure 8. It can be seen that = 7.0° yields a higher C_p, as there is a higher

Figure 7: C_p for One Pair Protrusion (= 5.7°)

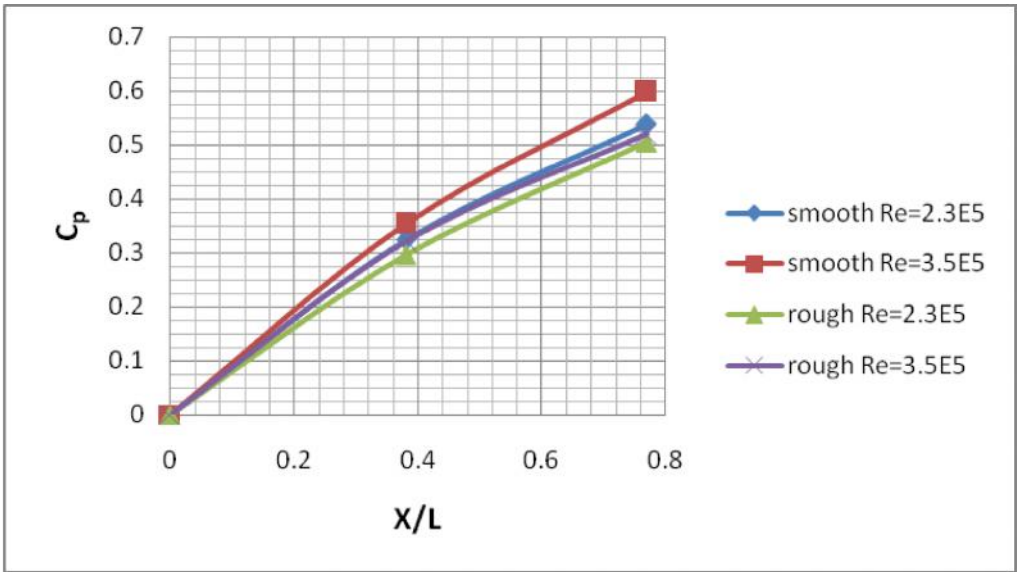

Figure 8: Comparison of C_p for Different

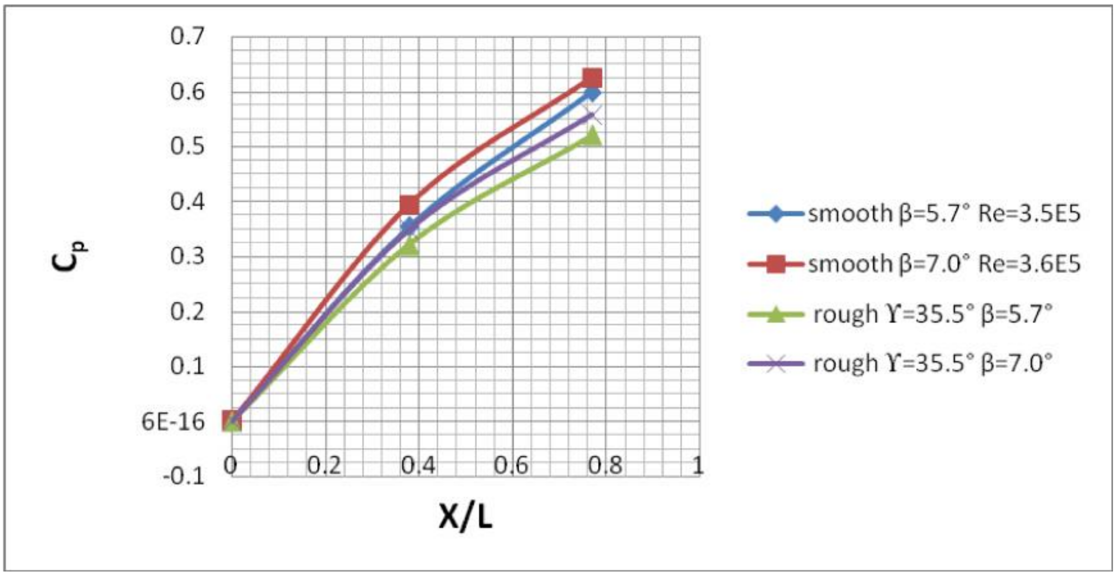

pressure rise in that case. The rough cases have a lower C_p than the smooth ones, due to increased losses.

The comparison of C_p variation, for the smooth and rough cases for = 5.7° for one and two pair VGs at different Re, is presented in Figure 9.

It can be seen that the smooth case yields the highest value at exit. This is due to the smooth configuration having minimum losses. The loss (as a function of inlet dynamic pressure) decreases with Re. This results are in C_p increasing with Re. The one pair VGs has a higher C_p than the two pair

Figure 9: Comparison of C_p for One and Two Pair VGs

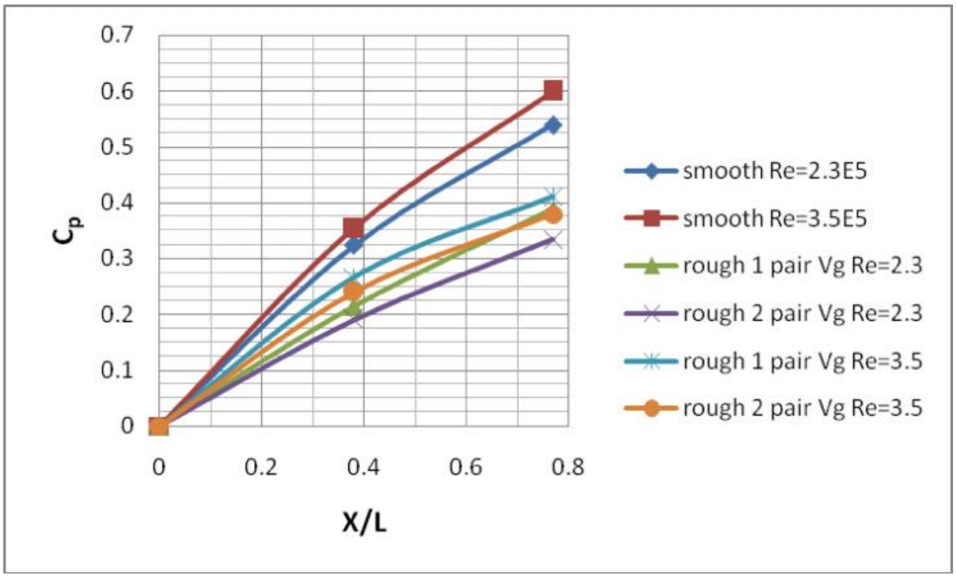

Figure 10: Variation of C_p for One Pair VG (Re = 3.5E5)

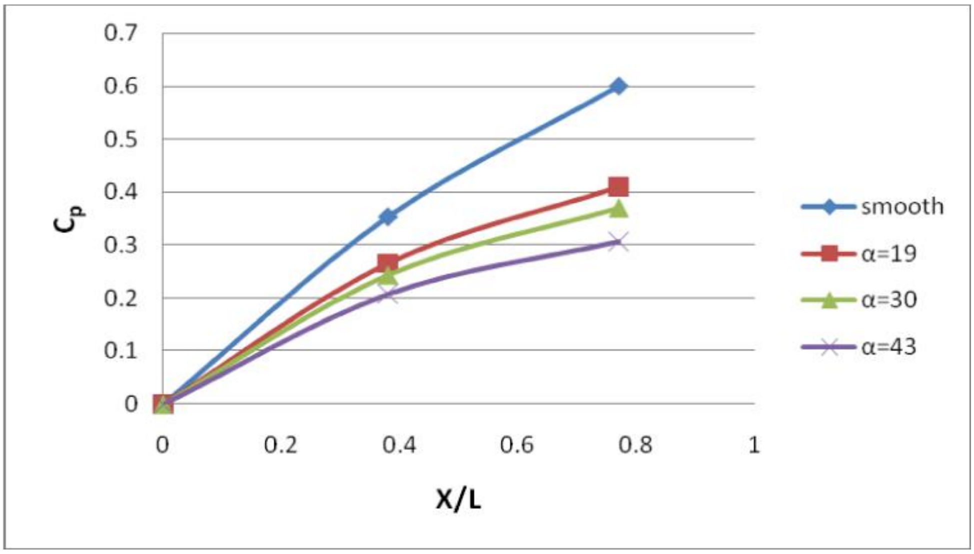

case due to the former experiencing lower losses.

The variation of C_p with for one pair VGs is shown in Figure 10.

As ~ increases, the pressure losses increase, leading to a lower C_p. The smooth case has the highest C_p.

The variation of C_p respect to the effect of diffuser angle is given in Figure 11.

The diffuser with = 7.0° has a higher C_p, as the pressure rise is higher.

Average Skin Friction Coefficient

The average skin friction coefficient is computed by performing momentum balance

Figure 11: Variation of C_p with =(One Pair VG)

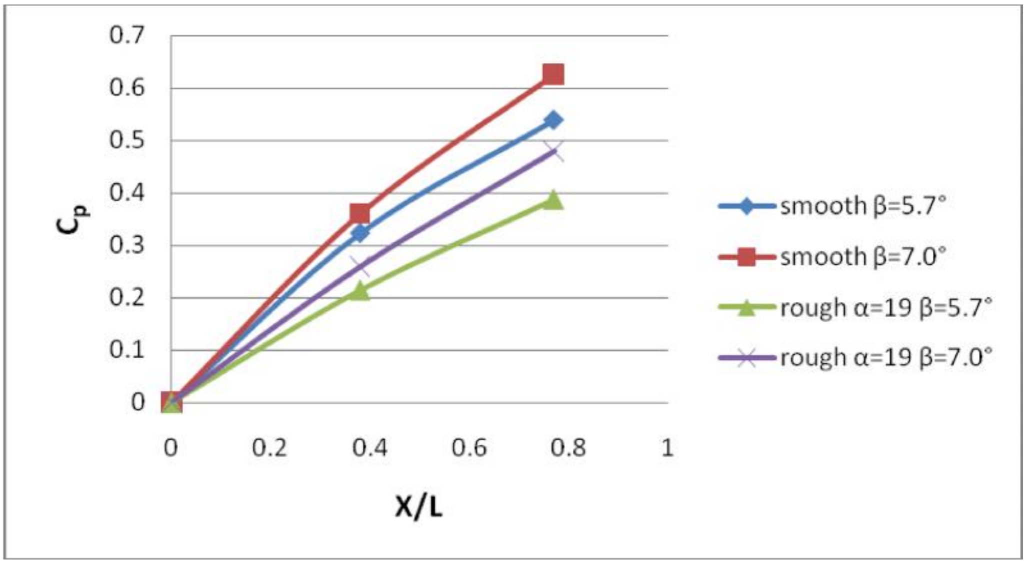

across the diffuser. The average skin friction coefficient is defined

$$C_f = \frac{2_w}{\frac{1}{2}\,{}^\circ V_{in}^{2}} \quad ....(1)$$

where,

$$2_w = \frac{F_{visc}}{A_{total}} \quad ...(2)$$

A_{total} is total area of all sides.

$F_{viscous}$ is defined as

$$-{}^\circ V_{in}^{2} A_{in} + {}^\circ \iint V^2\,dA = P_{in}A_{in} - P_{out}A_{out} + F_{viscous} \quad ...(3)$$

The variation of average skin friction coefficient is computed by performing

Figure 12: Average Skin Friction Coefficient (= 5.7°)

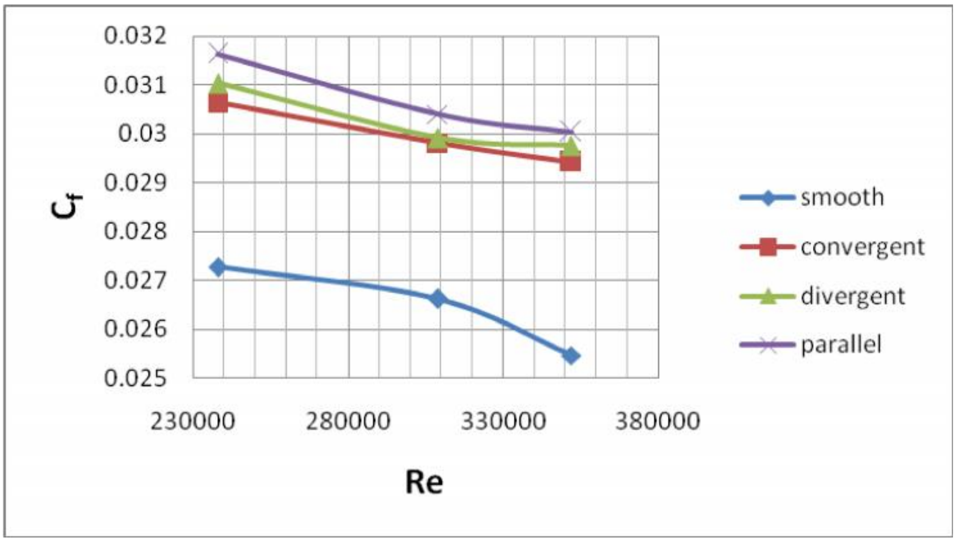

Figure 13: Average Skin Friction Coefficient (= 7.0°)

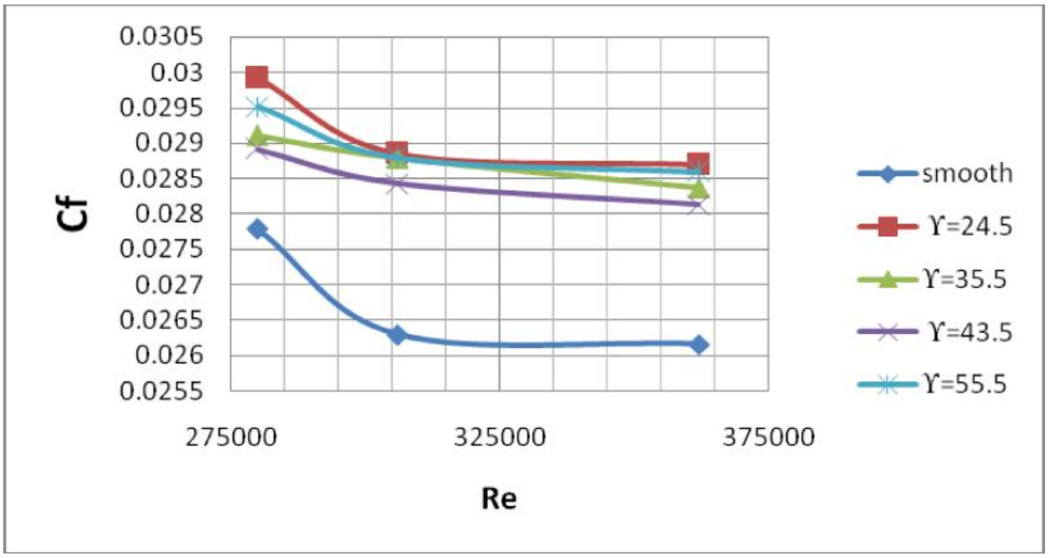

momentum balance across the diffuser. The variation of the average friction coefficient with Re for one pair protrusions is presented in Figure 12. The variation is for the smooth, convergent, divergent and parallel cases for the diffuser with half-angle   = 5.7°.

The variation of C_f is as expected. The increase in C_f in the rough case is due to the flow becoming turbulent. Three dimensional effects are strong and hence the average skin friction factor is higher. It can be seen that C_f decreases with Re for all cases. This is due to the losses (as a fraction of inlet dynamic pressure) decreasing with Re. The C_f has a higher value for the parallel case and is a minimum for the convergent one.

Figure 14: Average Skin Friction Coefficient (= 5.7°)

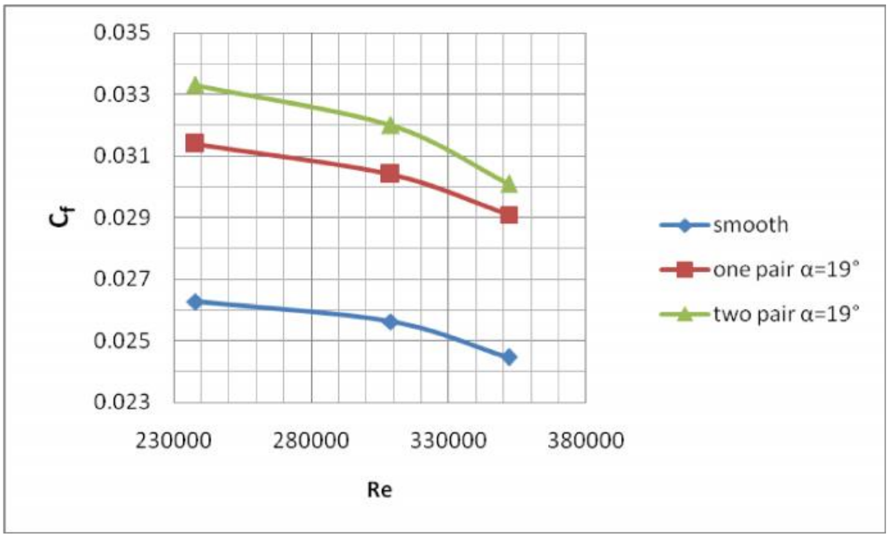

Figure 15: Average Skin Friction Coefficient (= 7.0°)

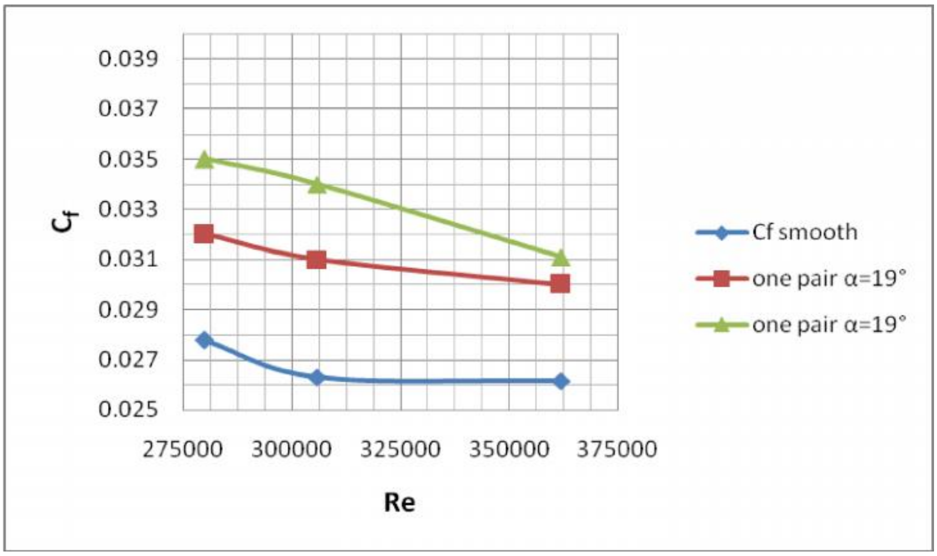

The variation of the average friction coefficient with Re for the different convergent angles of the protrusion, for the diffuser with = 7.0° is presented in Figure 13.

The trend is similar the previous one. It can be observed that C_f decreases with ¥(convergent angle). This implies that at higher values of protrusion angle (¥), the vortices created by the protrusion energise the boundary layer and thus minimise losses.

The variation of the average friction coefficient with Re for one and two pair VGs for different angles of diffuser are presented in Figures 14 and 15.

It can be seen that the diffuser with a higher angle ( ) yields a higher skin friction coefficient. This is due to higher stagnation pressure losses associated with the increased adverse pressure gradient. Similar to the previous case, C_f decreases with Re. One can also see that the two pair case has a higher C_f due to higher losses associated with the second pair.

CONCLUSION

The pressure coefficient cp increases with Re. The C_p value is lower for the rough case, due to increased losses. The diffuser with a higher angle attack yields a higher C_p.

The skin friction coefficient C_f decreases with Re for all cases. The value is higher for the parallel protrusion pair and is a minimum for the convergent one. The value of C_f decreases with increase in convergent angle. The skin friction coefficient increases with the diffuser angle , due to the increased adverse pressure gradient.

REFERENCES

1. Biswas G and Chattopadhyay H (1992), "Heat Transfer in a Channel with Built-in Wing-Type Vortex Generators", *International Journal of Heat and Mass*, Vol. 35, pp. 803-814.
2. Biswas G, Mitra N K and Fiebig M (1989), "Computation of Laminar Mixed Convection Flow in a Channel with Wing-

Type Built-in Obstacles", *Journal of Thermophysics*, Vol. 3, No. 4, pp. 447-453.

3. Fiebig M, Brockmeier U, Mitra N K and Guntermann T (1989), "Structure of Velocity and Temperature Fields in Laminar Channel Flows with Longitudinal Vortex Generators", *Numerical Heat Transfer*, *Part A*, Vol. 15, pp. 281-302.
4. Sohankar A (2007), "Heat Transfer Augmentation in a Rectangular with Vee-Shaped Vortex Generators", *International Journal Heat and Fluid Flow*, Vol. 28, pp. 306-317.
5. Tiggelbeck S, Mitra N K and Fiebig M (1992), "Flow Structure and Heat Transfer in a Channel with Multiple Longitudinal Vortex Generators", *Experimental Thermal and Fluid Science*, Vol. 5, pp. 425-436.
6. Tiggelbeck S T, Mitra N K and Fiebig M (1993), "Experimental Investigations of Heat Transfer Enhancement and Flow Losses in a Channel with Double Rows of Longitudinal Vortex Generators", *International Journal of Heat and Mass Transfer*, Vol. 36, pp. 2327-2337.
7. Von Stillfried F, Wallin S and Johansson A V (2011), "Evaluation of a Vortex Generator Model in Adverse Pressure Gradient Boundary Layer", *AIAA of Journal*, Vol. 49, pp. 982-993.